Environmental Impact Assessment Review 106 (2024) 107525

Contents lists available at ScienceDirect

Environmental Impact Assessment Review

journal homepage: www.elsevier.com/locate/eiar

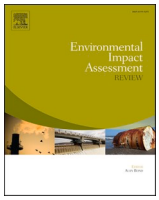

Optimal design of electromagnetic field exposure maps in large areas

P.L. López-Espí *, R. Sánchez-Montero, J. Guillén-Pina, R. Chocano-del-Cerro, J.A.M. Rojas

Departamento de Teoría de la Señal y Comunicaciones, Universidad de Alcalá, Escuela Politécnica Superior, 28805 Alcalá de Henares. Spain

ARTICLE INFO

Keywords:
Risk assessment
Exposure map
Electromagnetic pollution
Kriging

ABSTRACT

The mapping of electromagnetic field (EMF) exposure over large areas is a very useful tool for the analysis of epidemiological data and risk assessment. Its production requires a costly measurement process. To optimize the effort and ensure the representativeness of the exposure map, criteria for the selection of the sites to be measured must be established. This paper presents a methodology for conducting EMF exposure maps suitable for risk assessment evaluation in large areas. The proposal combines radio wave propagation criteria and GIS methods to optimize the sampling effort. The design criteria are based on the determination of a rectangular grid of 250 m side and the identification of the emitters within the area under study. Both urban and rural sites are analysed in the proposal and line of sight conditions (LOS) are considered to reduce the number of points required and thus optimize the measurement effort. Depending on the extent and regularity of the surface, the density of measurement points has been estimated to be between 8 and 10 points per square kilometre in the urban area. The proposed methodology has been applied to a case study of a 2.8 km^2 urban area within a 35.11 km^2 municipality, obtaining an average point density of 9.64 points/km^2 in the urban area. The differences in exposure depending on the application of the criteria have been analysed by means of the statistical values of the sets and the subtraction of the maps generated using kriging techniques. According to our results, if LOS measurements are not properly incorporated, the mean value of the EMF is underestimated in the area under study.

1. Introduction

In the last decades, due to the development of the Information and Communication Society, there has been an increase in exposure to electromagnetic fields (EMF), in particular those used by communication networks (mobile telephony, WiFi, wireless, etc.) and mainly in the radio frequency (RF) bands (Neubauer et al., 2007). At the same time, there has also been increasing public concern about the potential effects of EMFs, including RF and Low Frequency (LF) and on human health and biodiversity (Röösli et al., 2010; Biasotto and Kindel, 2018). The risk perception of these developments is complex and requires tools that provide the public with objective and easily understandable data (Wang et al., 2021). Radio propagation in urban environments is complex to calculate accurately and models and methods that try to assess the effect of multipath on radio propagation have been regularly used: Artificial Neural Networks, Radial Basis Functions… (Jawad et al., 2014; Aerts et al., 2013; Cansiz et al., 2016). From the beginning of these studies, the exposure assessment tried to analyse three aspects: What is the increase when incorporating a new station? What is the optimal way to measure exposure? And what is the biological effect produced? (Thuróczy et al., 2008) This work attempts to find the criterion to determine the amount of measures necessary to adequately assess the exposure in a large area, contributing to answering the second question.

There are two types of measurement procedures for monitoring RF field exposure: mobile (personal) and fixed. Fixed locations measured with a spectrum analyser or a frequency selective meter are the most accurate, although they require more effort in terms of cost and personnel. For a quick characterisation at a fixed location, there is also the possibility of using a broadband probe, although in the latter case, the spectral information specific to each service or the changes associated with the use of the RF spectrum, which is provided by personal exposure meters or measurements with selective meters, is lost (Sánchez-Montero et al., 2017).

General-purpose spectrum analysers additionally need an omnidirectional antenna and, in most cases, some additional programming that performs the averaging of the measurement is required. The selective meters for fixed sites have an integrated specific probe and are designed in such a way that they incorporate the classic averaging functions. Personal exposure meters allow a large number of measurements to be collected for a single individual or a population group. However, they

* Corresponding author.
E-mail address: pablo.lopez@uah.es (P.L. López-Espí).

https://doi.org/10.1016/j.eiar.2024.107525
Received 4 February 2024; Received in revised form 28 March 2024; Accepted 22 April 2024
Available online 27 April 2024

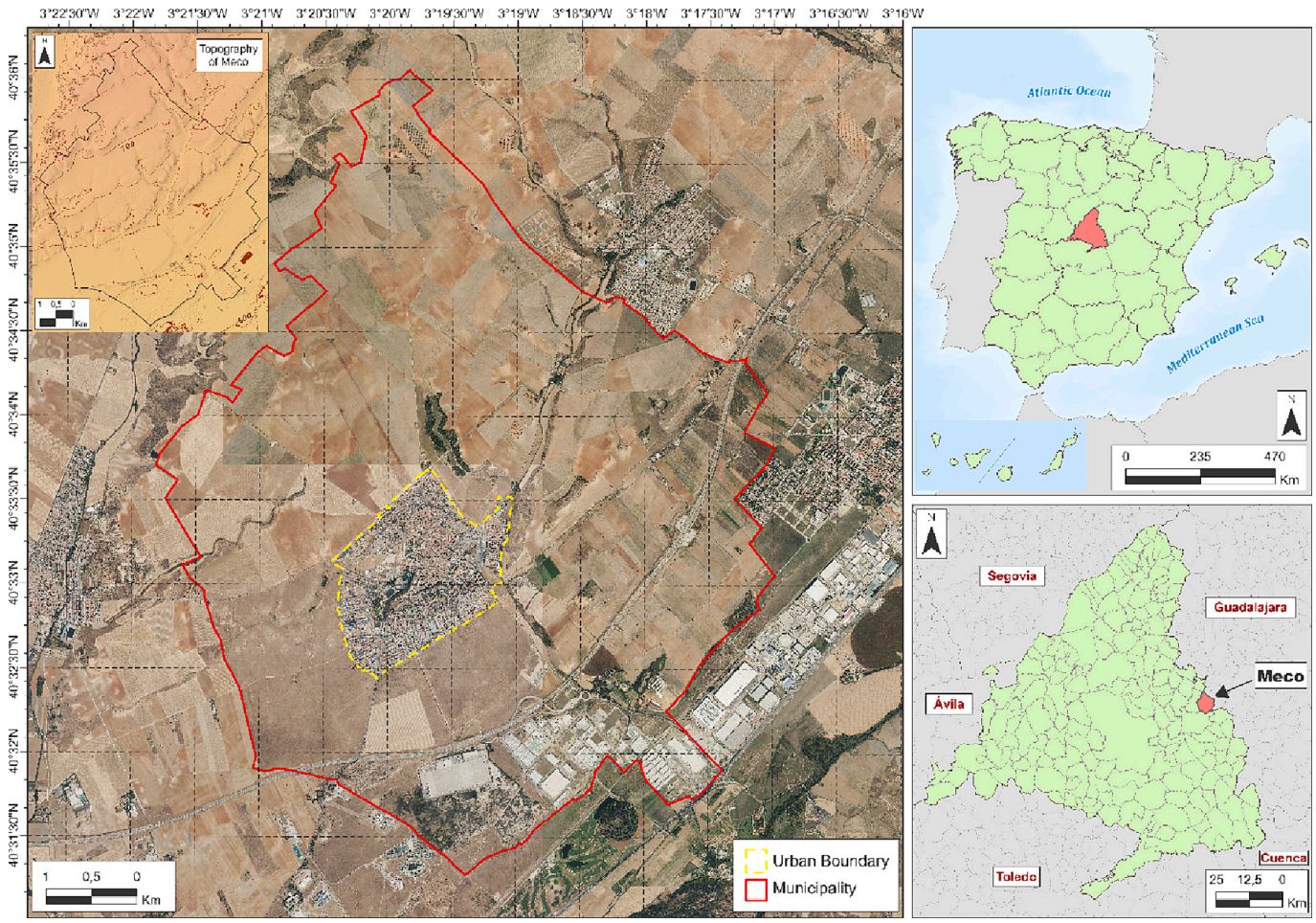

Fig. 1. Location of measurement area.

Table 1
Properties of the different analysed datasets.

Dataset	Point #	LOS #	Density (points/km^2)	Distance (m)
Urban	65	13	23.21	167.2
Urban 1	17	3	6.07	348.3
Urban 2	16	3	5.71	302.4
Urban 3	16	3	5.71	358.8
Urban 4	16	4	5.71	325.8
Rural	119	63	3.68	417.9
Rural 5	49	26	1.52	709.4
Rural 6	70	37	2.17	561.2
Urban 12	33	6	11.79	222.2
Urban 13	33	6	11.79	215.5
Urban 14	33	7	11.79	199.5
Urban 23	32	6	11.43	188.2
Urban 24	32	7	11.43	188.9
Urban 34	32	7	11.43	221.1
Urban 123	49	9	17.50	179.7
Urban 124	49	10	17.50	178.7
Urban 134	49	10	17.50	186.0
Urban 234	48	10	17.15	170.4

present the problem of generalising the results, although the mobility of the user, as an element to be considered in the exposure, makes them particularly interesting in the analysis of spatial variation for a single user. Up to now, to ensure the adequacy of the EMF exposure levels at a site to the current regulations, two methods are recommended indistinctly: measurements with a selective meter or spectrum analyser and broadband measurements. Both are based on the ICNIRP original guidelines from 1998 (International Commission on Non-Ionizing Radiation Protection (ICNIRP), 1998), EN50413 and IEC 62311 (International Electrotechnical Commission, 2019), on which the European and Spanish regulations are sustained (BOE, 2001; BOE, 2002; European Union, 1999). Recently, ICNIRP has published an update of the recommendations on EMF protection (International Commission on Non-Ionizing Radiation Protection (ICNIRP), 2020). Among the most notable changes affecting this work are the change of the averaging interval to 30 min (as opposed to the previous 6 min) for the whole body and the limit up to 2 GHz in the definition of the reference values. The most restrictive limit is 27.7 V/m in that bandwidth, versus 28 V/m in the probe bandwidth (100 kHz to 3 GHz) considering the 1998 recommendations. In the case of local exposures, the averaging interval can be greater than or equal to six minutes and is also considered up to 2 GHz. Its most restrictive value in the bandwidth is 62 V/m. These changes have not yet been incorporated into the aforementioned European and Spanish regulations. For this reason, and for reasons of comparison with previous work, the measurements made in this proposal have been averaged over a 6-min interval.

Until the recent incorporation of geostatistical techniques that have made it possible to characterise large areas, the adequacy of radio levels using fixed sites was usually restricted to the legally required measurement of levels near mobile phone base stations (BTS). In this context, the portable personal exposure meters appeared and have allowed the development of numerous studies to characterise RF-EMF exposure in several European cities (Gajšek et al., 2013; Sagar et al., 2018). Personal exposure meter studies developed in the last decade have allowed the characterisation of the personal exposure and the prediction of exposure levels through the development of models (Frei

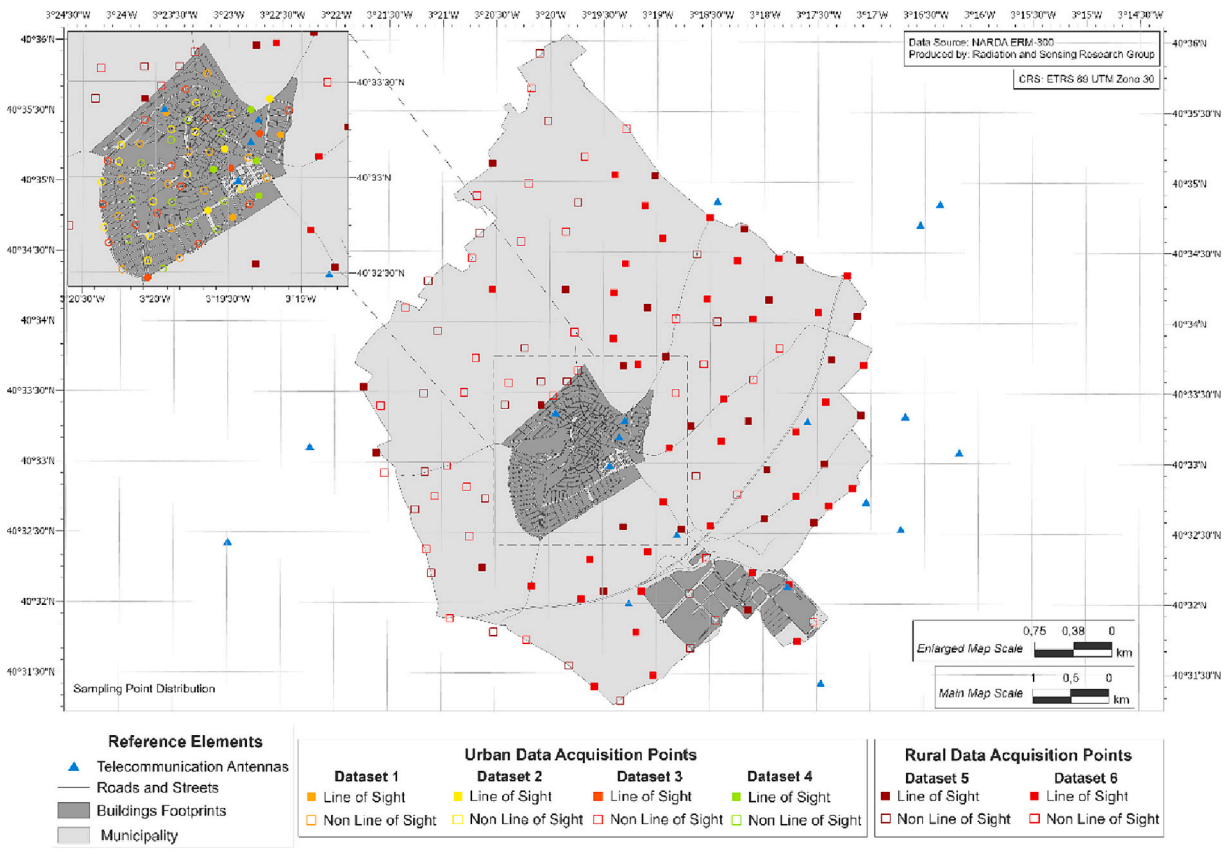

Fig. 2. Location of the measurement points for different subsets.

Table 2
Statistical values of the measured datasets in urban and rural areas.

	Count	Average	Standard deviation	Minimum	Maximum	Range
Urban 1	17	0.329	0.475	0.05	1.90	1.85
Urban 2	16	0.153	0.110	0.04	0.45	0.41
Urban 3	16	0.260	0.307	0.06	1.22	1.16
Urban 4	16	0.250	0.243	0.06	0.96	0.90
Urban	65	0.249	0.315	0.04	1.90	1.86
Rural 1	49	0.216	0.164	0.05	0.66	0.61
Rural 2	70	0.241	0.210	0.03	1.00	0.97
Rural	119	0.231	0.192	0.03	1.00	0.97

et al., 2009; Beekhuizen et al., 2013; Beekhuizen et al., 2014; Martens et al., 2016), compare personal exposure in different cities (Urbinello et al., 2014a), verify compliance with legal limits (Urbinello et al., 2014b) or study spatio-temporal differences (Vermeeren et al., 2013; Viel et al., 2011). They have also been used to characterise singular events such as concerts or fairs, where temporary installations and large number of people occur (Ramirez-Vazquez et al., 2019). Its main advantages are small size, sensitivity and the ability to store large amounts of data. This makes them especially suitable for the assessment of microenvironments. The main drawback of personal exposure meters in this case is the extrapolation of the data obtained individually, especially in terms of adapting to EMF exposure legislation. Another important issue is the bias of the measurements (Bolte, 2016). Because of this, they tend to underestimate the value of the measurement (Najera et al., 2018). These devices measure specific bands, but not the entire bandwidth. They are also not suitable for near-field measurements and their measurement refers to local exposure on the body. For this reason, when assessing levels over large areas, a method with fixed locations is preferable (Sánchez-Montero et al., 2017).

Broadband measurements enable a global characterisation of the radio environment and have been used to verify levels, find emission sources, etc. (Koppel et al., 2022). In some cases, characterisation has been limited to trajectories in order to find the maximum values in an area (Liu et al., 2019), around a single base station or in a street (Pachón-García et al., 2014). They have also been used to obtain the relationship between indoor and outdoor measurements (Reis et al., 2018).

Different geospatial methods (Spline, Inverse Distance Weighting (IDW) and kriging) have been used to plot electric field variations from fixed site measurements on a map (Bojdova et al., 2019; Giliberti et al., 2009). The Kriging method performs optimally for wide ranges of values, while the IDW works best for small values. The kriging technique has been widely used for risk assessment and representation of environmental variables combining remote sensing techniques and local sampling in flood prevention or agriculture (Kross et al., 2022). The Kriging technique has been applied to interpolate small areas with high sampling densities (Iyare et al., 2018), or even to calculate the specific absorption rate in the human body. Obtaining a general value of the exposure is of crucial importance when it comes to relating this data to the appearance of certain diseases (Gonzalez-Rubio et al., 2017). Obtaining particular solutions can lead to errors in establishing incidence relationships (Gonzalez-Rubio et al., 2016). The aim of this work is to determine the optimal criterion for the choice of fixed measurement sites to determine the EMF exposure over a large area using Kriging techniques.

Section 2 describes the materials and methods used in carrying out this proposal. First, a description of the environment in which the measurements were taken is given, presenting the points in two different areas: rural and urban. These points have been grouped to obtain

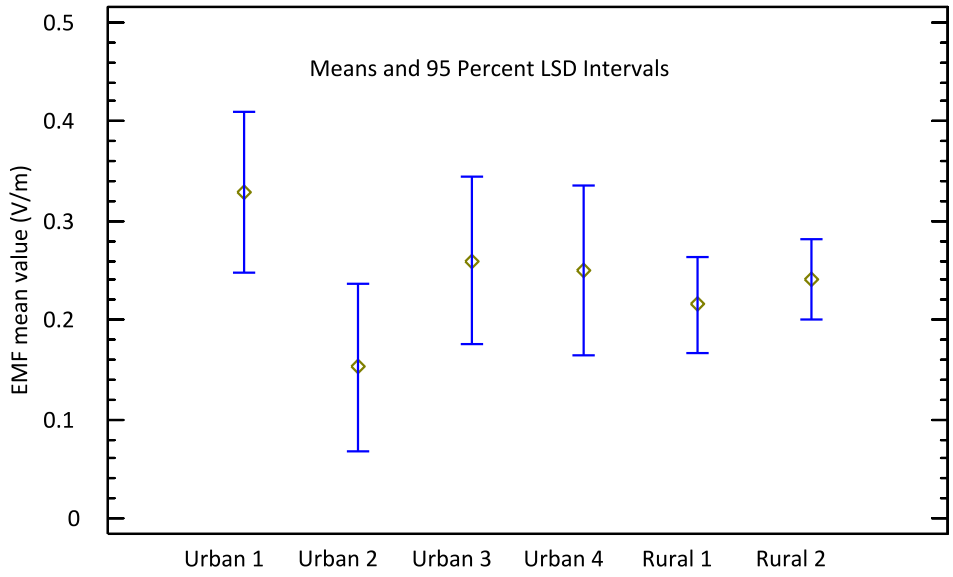

Fig. 3. Means and confidence intervals for urban and rural data subsets.

Table 3
Statistical comparison between different datasets.

Comparison	p-Value
Urban 1 / Urban 2	0.0000
Urban 1 / Urban 3	0.0992
Urban 1 / Urban 4	0.0130
Urban 2 / Urban 3	0.0003
Urban 2 / Urban 4	0.0040
Urban 3 / Urban 4	0.3760
Rural 1 / Rural 2	0.0694

coverage densities and distances in the urban area in the range of 23.2 to 5.7 points/km^2 and 167.2 to 358.8 m. In the rural zone, densities and distances range from 3.68 to 1.52 points/km^2 and 417.9 to 709.4 m. These values make it possible to discuss in a wide range, depending on the characteristics of radio propagation, the effort of measurements to be made to obtain a true estimate of the exposure values. This section also describes the equipment used to make the measurements, in this case a NARDA EMR 300 m, and the protocol used to make the measurements. The subsequent analyses are based on the calculation of the statistical values of the different data sets (mean, variance, distribution fit and independence) and their appropriate geographic interpolation. The software tools used for this purpose (Statgraphics, ArcGIS and QGIS) have also been expressly mentioned in Section 2. Finally, the validation of the proposals has been carried out by comparing them with additional measurement campaigns. The characteristics of these campaigns have also been described in Section 2. Section 3 analyzes the statistical properties of the different data sets. This has allowed us to discard as the only criterion in the definition of the number of measurements required the distance between points or the density of points, while introducing the visual watershed analysis to distinguish the 250 × 250 m^2 grids according to their surface under LOS or non LOS (N-LOS) conditions. To argue the insufficiency of measurements in the case of 500 × 500 m^2 grids, the additional campaign carried out with this criterion has been analysed, testing the shortcomings of the geographic interpolation. Section 4 discusses the characteristics of the different measurement subsets that may lead to errors in the geographical representation, and then establishing the necessary criteria to be fulfilled for the adequate representation of the exposure: existence of measurements in LOS conditions, measurements in the contours of the surface to be measured to avoid errors in the limits of the exposure maps and the possibilities of reducing the number of measurements according to LOS/N-LOS conditions. According to this discussion, a proposal for an optimal measurement campaign has been made with a density of 9.64 points/km^2 in the urban area, which has been contrasted with the 4 points/km^2 suggested by the regulations cited in the text. Finally, the conclusions drawn from this proposal are highlighted in Section 5 below.

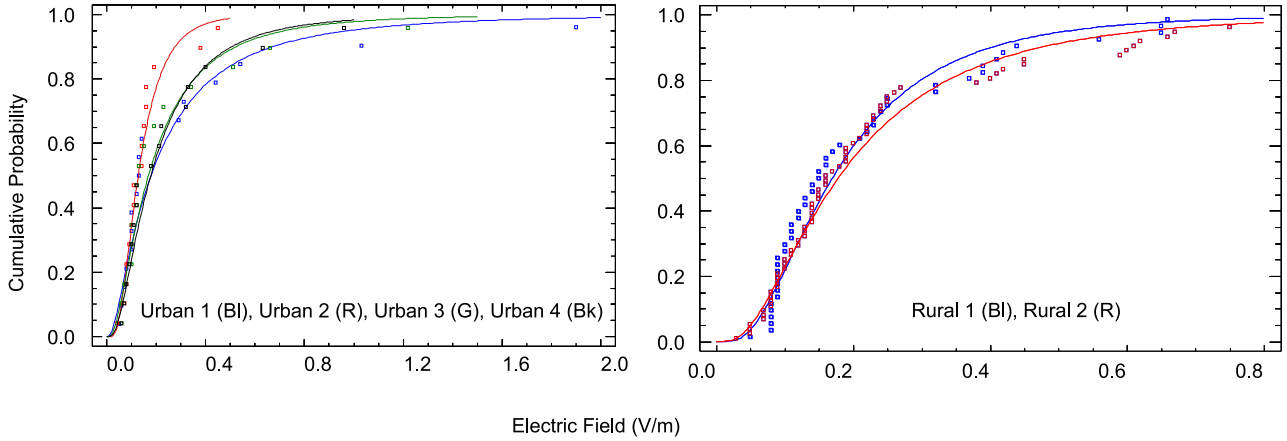

Fig. 4. Probability distributions for the different sets in urban (left) and rural (right) areas.

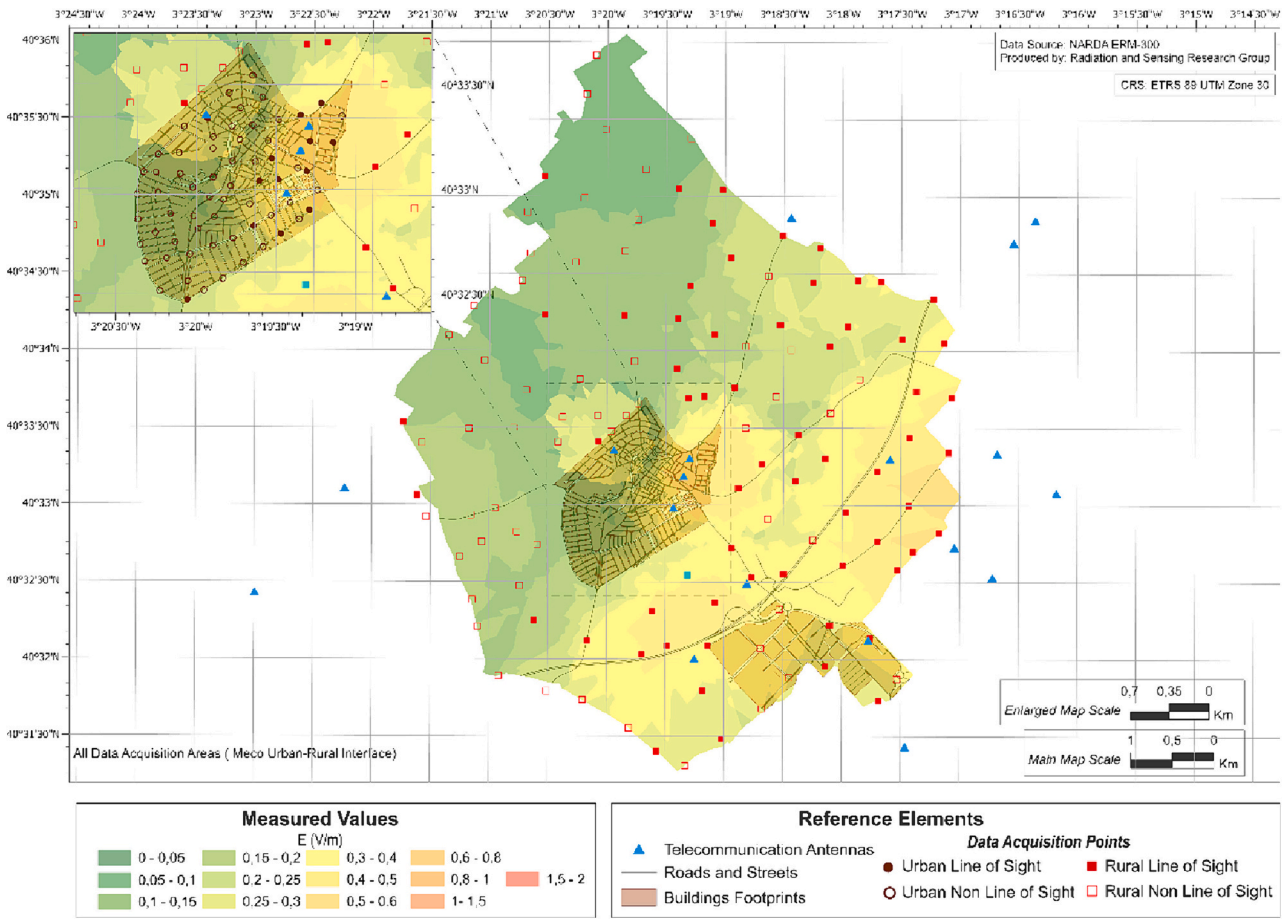

Fig. 5. Plot of measured values in urban (left) and rural (right) areas for the whole set of points.

2. Material and methods

2.1. Location of the measurement points

Meco is a municipality of about 13.000 inhabitants located about 30 km east of Madrid. The area of the municipality is 35.11 km^2 and can be divided into an urban area and a non-inhabited (rural) area. The urban area is well delimited and corresponds to an extent of 2.80 km^2. In the southern area, there is a small industrial area, far away from the urban area, which will not be considered in this study.

The council has the classic FM and DTV broadcasting services, although there are no transmitters within the municipality or in neighbouring areas. There is also mobile telephone coverage, for which there are eight BTS's within the municipality and another nine that provide service from neighbouring areas. The surface is generally smooth, with a higher elevation in the north, so there are no shaded areas due to the presence of natural obstacles. The location of the municipality is shown in Fig. 1. The solid red line delimits the municipal area, and the yellow dashed line determines the urban area. The topography of the terrain is also shown in the upper left corner of Fig. 1.

ITU-T recommendation K.113 (International Telecommunication Union. Recommendation ITU-T K.113, 2015) suggests establishing grids of no >500 m (4 points/km^2) used to divide up the surface area and take measurements at its corners. In an area such as the one described above, this implies taking approximately 140 measurements over the entire municipal area, of which approximately eleven would correspond to the urban area and the remaining 129 would correspond to the rural area. The establishment of precise grids in urban areas, when the intention is to take measurements at street level according to the ICNIRP criteria (International Commission on Non-Ionizing Radiation Protection (ICNIRP), 2020), is practically impossible due to the inaccessibility of them. Regarding the distances between measurements, in (Thuróczy et al., 2008) distances of up to 250 m were taken with respect to the BTS in an urban environment. Due to the characteristic of radioelectric propagation, a relationship between distance and exposure levels was not established. According to previous works (Sánchez-Montero et al., 2017; Najera et al., 2018) acceptable results can be obtained when the distance range is around 250 m. When it comes to propagation in free space, the attenuation of the electromagnetic wave is directly proportional to the square of the distance (Friis Equation). This contribution is the most relevant in conditions of direct vision to the emitter (LOS). However, in the absence of direct vision (N-LOS) the received signal is the result of multiple reflections, in what is known as multipath. In this case, the signal is characterised by a variation with distance that differs greatly from Friis's law of quadratic variation and coverage calculations are usually obtained from empirical propagation models. So, it must be decided to locate the sites in accessible places, ensuring a homogeneous coverage of the area. In this work, a slightly larger set of points than initially suggested has been used as a starting point. To achieve coverage of the entire municipality, 184 measurements were taken, 65 (23.21 points/km^2) in the urban area and 119 (3.68 points/km^2) in the rural area. The measurement points have been chosen to achieve a homogeneous coverage of the terrain, considering the possibilities of access to the sites.

This implies in a practical way, as previously mentioned, the impossibility of establishing regular grids in the field. The recommendation does not explicitly state the obligation to take measurements at points with a direct LOS to the transmitters, however, as will be shown later, this criterion needs to be incorporated in the identification of the measurement points. In the maps produced, BTS's have been marked by

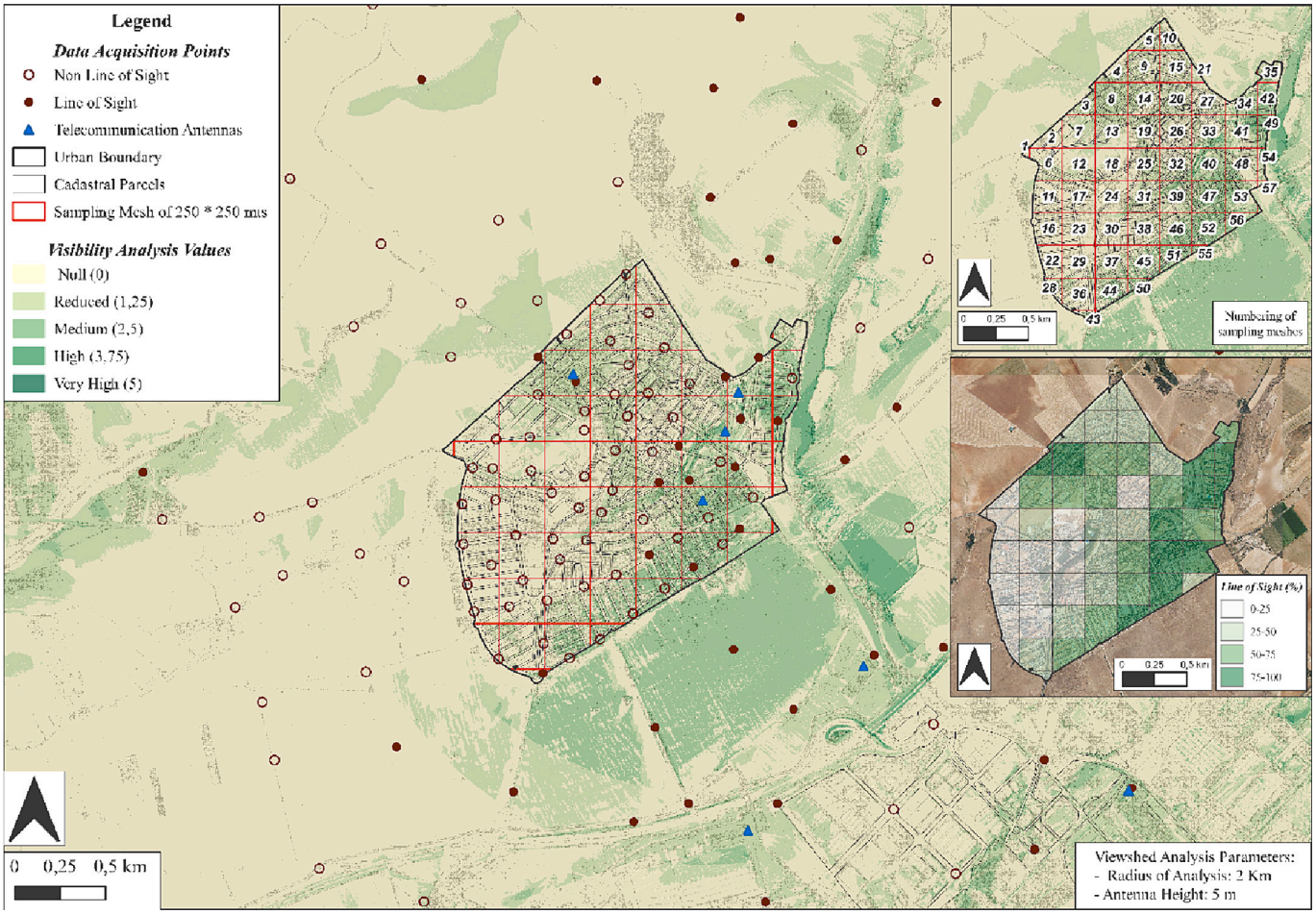

Fig. 6. 250 × 250 m^2 grids and visual viewshed analysis.

blue triangles. Solid symbols (squares or circles) represent measurements where direct LOS is achieved to any of the emitting sources. In contrast, hollow symbols (squares or circles) indicate measurement points where there is no direct line of sight (N-LOS).

The classification as rural or urban tries to distinguish cases where the radio propagation can be explained by a classical two-ray model (rural) or may be characterised by a multipath model due to the presence of buildings and other obstacles (urban). In the case under study, the buildings throughout the urban area correspond to residential houses of no >10 m in vertical height, except in an area in the southeast where there is a group of blocks of flats of approximately 20–25 m in height.

The initial point densities achieved, as previously indicated, in urban and rural areas are 23.21 points/km^2 and 3.68 points/km^2 respectively. The average distances to the nearest point are 167.2 m in the urban area and 417.9 m in the rural area. This is a slightly lower starting point than what was established in previous works. To determine the adequate point density in each area, the points in the urban area were divided into four subsets (dataset 1 to 4) and the rural points into two subsets (dataset 5 and 6). In addition, to study the influence of the density of points on the estimation of the measurements, the urban sets have been grouped in pairs or triplets so that they have average distances between similar points and form a homogeneous coverage network. The number of LOS points in each of the urban subsets has been chosen similar and in the rural sets, it has been chosen proportional to the total number of points.

Table 1 shows the number of points in each set and the average density and distance. The representation of the subsets of points is shown in Fig. 2 with the colours indicated below. For urban area measurements (circle): urban 1, urban 2, urban 3 and urban 4. For the rural area measurements (square): rural 5 and rural 6. Each of the four subsets has mean distances between 300 and 350 m. If the subsets are grouped in pairs, the average distances are approximately 200 m, whereas, if the grouping is done in triplets, the average distances range between 170 and 180 m. The two subsets in rural area have been chosen with different average distances, the first one with slightly >500 m and the second one with a value of >700 m. For example, in the case of urban sets, the urban12 pair contains the points of both subset 1 and subset 2. The urban123 trio contains the points of subsets 1, 2 and 3. When contrasting a group of points (subset, pair or trio) compared to others, the aim is to highlight the characteristics that differentiate it from the rest. Likewise, it is intended to check the validity of the interpolations for different distance ranges, using different sets of points that represent, with different distance and density, the exposure value. In this way, distances of approximately 160 m are compared in the case of all urban points, approximately 300 m when the single subsets are considered, about 200 m when the pairs are considered and around 180 when the trios are considered. Similarly, in the rural case, distance ranges between points vary in the range between 417.9 and 709.4 m depending on the group of points considered. The distribution of the points between the different subsets has been made to maintain approximately homogeneous surface coverage in all cases.

2.2. Measurement equipment and protocol

The measurement equipment follows ITU recommendations: a minimum detection level of 1 V/m, a dynamic range > 40 dB, linearity of 1.5 dB, probe isotropy <2.5 dB (International Telecommunication Union. Recommendation ITU-T K.100, 2021), minimum rms

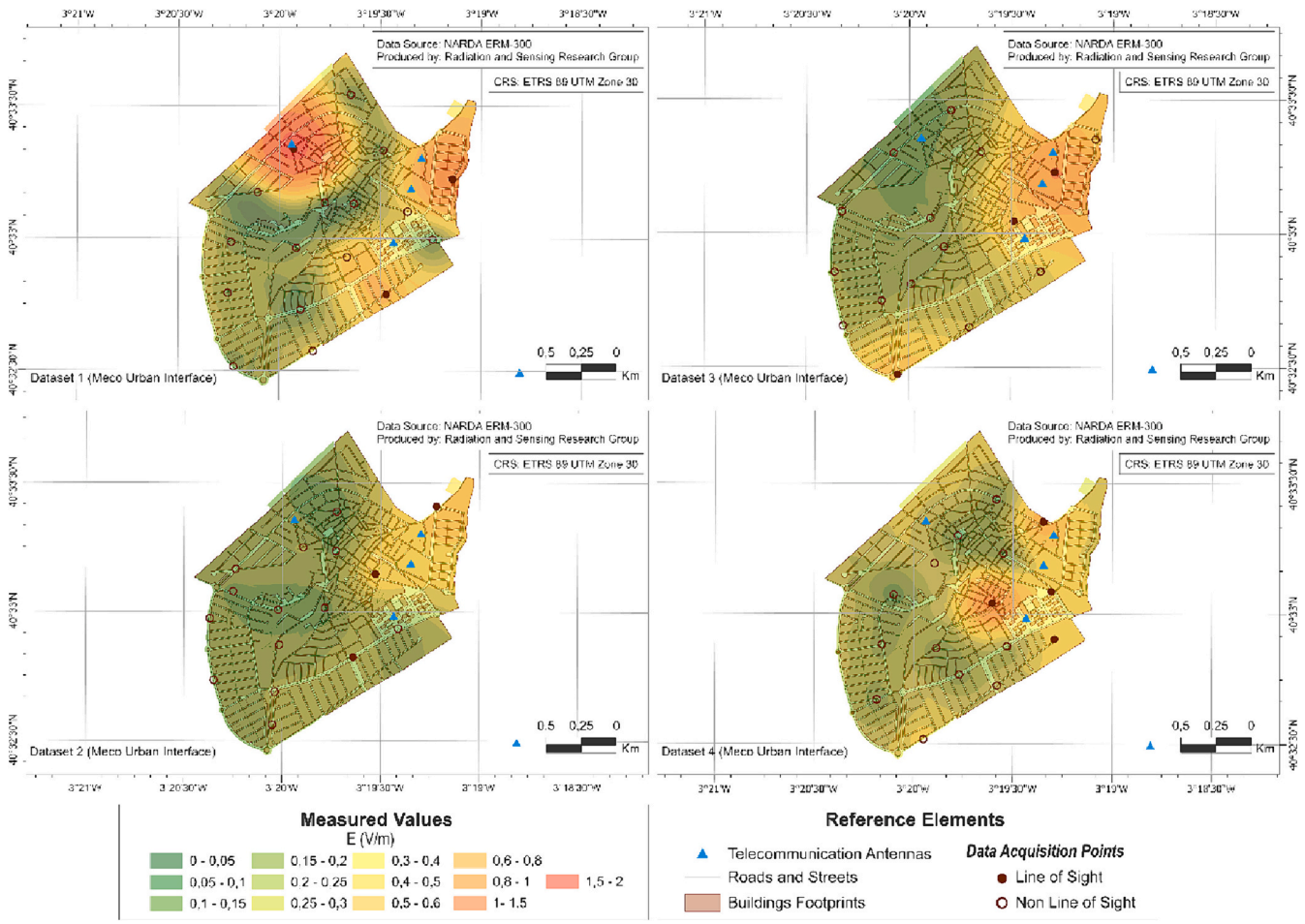

Fig. 7. EMF interpolation of the different urban datasets.

measurement range 0.3–20 V/m; and sensitivity 0.3 V/m (International Telecommunication Union, 2018; International Telecommunication Union, 2024). In our proposal, a Narda EMR-300 Broadband RF Survey Meter and a Narda Isotropic Probe 18C were used for the measurement of the electric field intensity in the 100 kHz to 3 GHz range with 0.01 V/m resolution, detection level of 0.2 V/m, a dynamic range of 60 dB, linearity ±0.5 dB, isotropic deviation ±1.0 dB, an rms measurement range of 0.2 to 320 V/m, a sensitivity 0.2 V/m. We also used a non-metallic Tripod EMCO 11689C. The parameter that determines compliance with the standard is the electric field level. According to current legal limits, the most restrictive value in the range is 28 V/m (please remember that this refers to ICNIRP 1998 version). Therefore, if the cumulative measured value is lower than this value, compliance with the standard is verified. In our case, the instantaneous measured values were automatically averaged for 6 min using the RMS mode of the device. To carry out the measurement, an open area has been selected within each of the chosen grids. In cases of direct vision (LOS), the line of sight with the different BTS has been ensured, avoiding shielding from walls, trees or other obstacles. The meter has been placed on the tripod at a height of 1.5 m and the rms averaging mode has been activated for 6 min. During the measurement, a distance of several meters from the equipment has been maintained and the use of electronic devices that could interfere with the measured value has been avoided. To ensure comparable use of the base stations, all measurements were taken during the 9:00 to 14:00 time slot from Mondays to Fridays.

2.3. GIS and statistical tools

ArcGIS Pro 3.0 (ESRI, 2016) was used to create the maps and QGIS 3.26 (Čučković, 2021) was used to obtain the viewshed analysis, which assessed the existence of direct vision to the different base stations. The methodology chosen for the geographical interpolation of exposure values has been ordinary kriging. This type of interpolation is the one that presents the best results compared to other types of kriging or the traditional inverse distance (IDW) technique (Sánchez-Montero et al., 2017). Statistical analyzes were carried out using Statgraphics (Statgraphics Technologies Inc, 2009) software. This package allows the performance of means, variances, comparison of sample independence and the fitting of points to different probability density functions.

2.4. Additional measurements campaigns

In addition to the sets of points indicated in Section 2.1, two additional measurement campaigns have been carried out in 2023. The first of them consisted of a set of 11 urban points with an average distance of approximately 500 m (3.93 points/km^2) with the objective of comparing the results of its interpolation with that obtained with the original set. This should allow us to validate or discard that original average distance between points as a sampling value for the territory. In the second campaign, also in 2023, 27 new urban points have been measured following the criteria obtained from the analysis of the original points (9.64 points/km^2). The objective of this latest campaign is to validate the proposed criteria, proving that there are a number of points that optimize the effort in data collection, maintaining the representativeness of the exposure values.

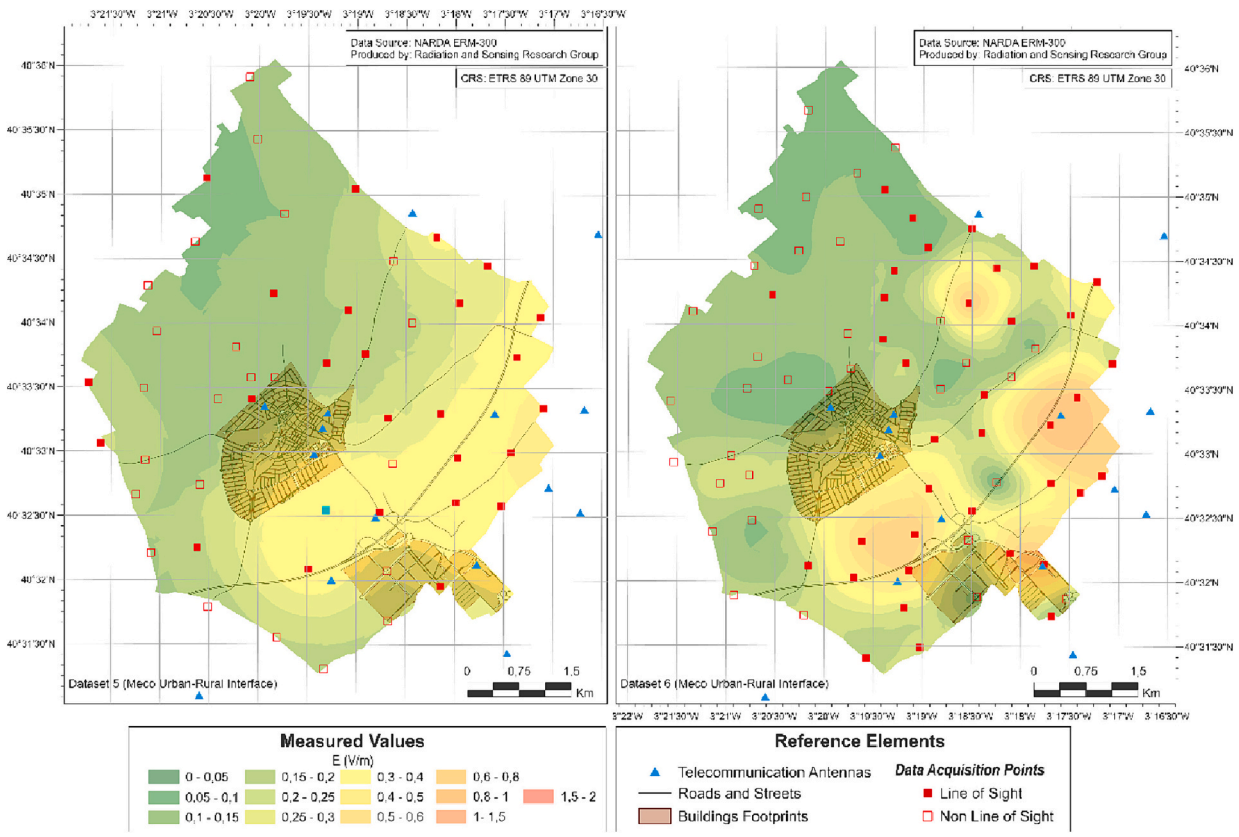

Fig. 8. EMF interpolation of the rural datasets.

3. Results

3.1. Statistical properties of the measured values

In this section, the main statistical values of the different sets and subsets of points will be analysed. First, we will compare the mean and variance values to check whether the different subsets have similar overall properties. A subset may be considered valid if its statistical properties represent with similar fidelity the global set. That is, if the average value of the urban or rural area within its confidence interval and its variability is similar for each of them. Secondly, the statistical differences between the subsets of values will be analysed. The existence of subsets independent of the rest will be an indication that their variability represents the surface under analysis differently and, therefore, the reason for these differences should be the subject of discussion. The last statistical tool used to characterise the subsets is the fitting of the probability function. This is a graphical way to visualize the statistical differences between different subsets. The statistical results of the carried-out measurements are summarised in Table 2 for the areas identified as urban and rural.

As can be seen from the tables above, the maximum values measured in both the rural and urban areas are well below the legal limit of 28 V/m. Before to validate the compliance of the whole area using the subsets, it is convenient to compare them statistically. For this reason, the main statistical values of the samples and their independence are analysed in the following. First, the values of the means and confidence intervals of the different sets are shown in Fig. 3. Analyses of the means, medians and standard deviation between the different urban sets or between both rural sets performed with Statgraphics (Statgraphics Technologies Inc, 2009) show that there are no significant differences between the means of these sets. Similar results are obtained for the median tests.

If a comparison is made between the standard deviation of the samples, Table 3 is obtained. In the cases where the p-value is <0.05, there is a statistically significant difference between the sets analysed. For the rural sets, no significant statistical differences were found in the mean, variance, and median tests. On the other hand, in the urban sets, there are no statistical differences in the mean and median, but there are differences in the variance.

As can be seen, in the urban area, even for average distances between points ranging from 300 to 350 m, which is far less than the 500 m, recommended by the ITU, there are significant statistical differences. On the other hand, in the rural area, for distances >500 m, there are no significant differences. From these results, it can be established that the average distance between points (or their density) cannot be considered as the only criterion for selecting the measurement points. If the distance were the only criterion, independent subsets should represent the exposure values in a similar way. For this reason, it is necessary to analyse the origin of these differences between the sets to propose an optimal criterion for performing this type of measurements.

According to previous work (Cansiz et al., 2016; Sánchez-Montero et al., 2017), the measurements follow a lognormal statistical distribution. Fig. 4 shows the cumulative probability plots for the different clusters. In the case of the urban sets, the colour assignment is Blue-1; Red-2; Green-3; Black-4. In the case of the rural sets, the colour assignment is Blue-1; Red-2. As can be seen in the figure, urban subset 2 (red), which has the lowest mean of the four, is the one that visually shows the greatest differences compared to the rest of the sets.

For a better understanding, a representation of the measured levels has been made using ArcGIS (ESRI, 2016). The interpolation technique chosen, in accordance with the literature cited, was ordinary stable kriging. To establish a valid comparison between the representations, the following parameters have been set for all of them: Output cell size: 0.5, Search Radius: Variable and Number of points: 12. The measurements with the highest value correspond to the areas close to the BTS's where there is a LOS between the measurement point and the transmitting antenna. Conversely, the lower value measurements occur in

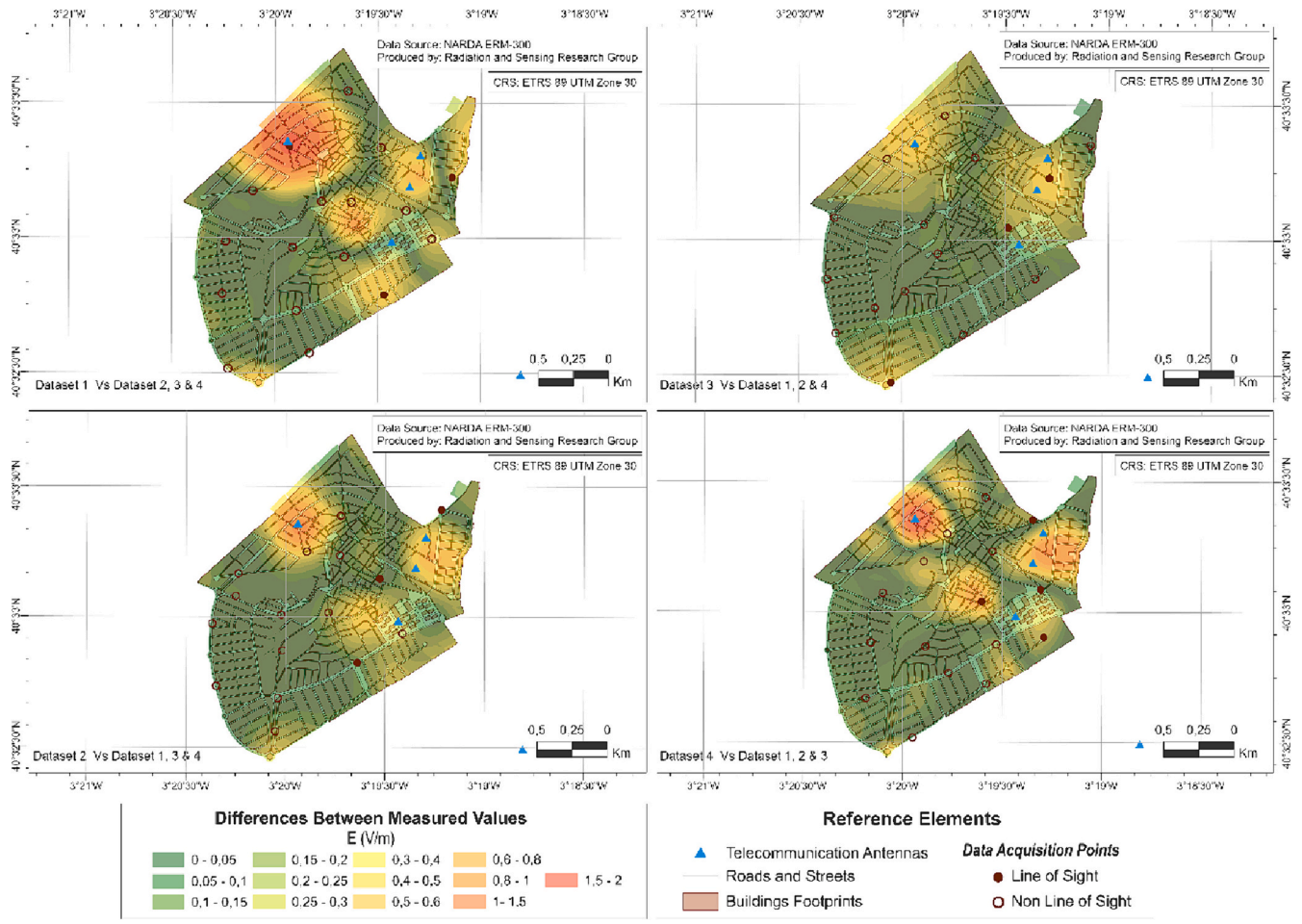

Fig. 9. Differences between a dataset and the other three.

areas further away from the BTS's or where there is N-LOS to the antenna. Fig. 5 represents the interpolation over the entire municipal area. In all the maps made, for the sake of comparison, a single scale of values between 0 and 2 V/m divided into 13 intervals has been used.

3.2. Definition of the grid and measurement criteria

In the previous maps, the areas with a higher level of exposure are near the BTS. As indicated above, the existence of direct vision conditions (LOS) to them presupposes the existence of a higher level of exposure. On the contrary, the lack of these measurements would lead to underestimating the real values and, therefore, obtaining lower averages. To assess the influence of LOS condition on the measured EMF levels, a visual viewshed analysis of the municipality has been carried out. Fig. 6 represents a visual viewshed analysis of the urban area from the emitting sources, based on digital elevation mapping of the terrain, including buildings, considering a height of 5 m for the BTS antenna and a maximum visual range of 2 km. This analysis has been carried out using the Visibility Analysis plug-in of QGIS (Čučković, 2021). In Fig. 6, grids of half the value of the ITU-T K.113 recommendation, i.e. 250 × 250 m^2, have been included. Fifty-seven grids have been identified, although six of them have an almost negligible area. The darker areas represent direct vision and closer proximity to the emitting sources. Lighter areas indicate greater distance to the emitting source or N-LOS. Areas with higher visibility are mainly located to the south and east of the urban area. The western area is the area that contains the largest shaded area. Based on the percentage of direct vision surface in each grid, in the inner map, the grids have been classified in four intervals.

To discuss the criteria for the assessment of the optimal number of points or to characterise of the set of measurements that make it statistically representative, the measured data have analysed in terms of the six subsets indicated in Table 1. The interpolation of the measurements obtained by kriging techniques is depicted in Fig. 7 and Fig. 8. Fig. 7 corresponds to the four urban subsets and Fig. 8 corresponds to the two rural subsets. This reduction of points in the different subsets implies that there is no direct vision measurement in the vicinity in some of the emitting sources. This effect can be appreciated in subset 2 of Fig. 7, where the absence of line-of-sight points leads to an almost homogeneous estimation over the whole area.

To highlight the differences between the different subsets, subtractions have been made between the maps shown in Fig. 7 and Fig. 8. The analyses have been made, in the urban case, by comparing them in pairs or individually with respect to the other three. The differences have been obtained using map algebra. For example, to compare the points of subset 1 with the rest of the urban points, interpolation maps have been made with the points of subset 1 (Fig. 7 upper left) and with the set of points of the trio formed by subsets 2, 3 and 4 (not shown in the figures to avoid redundant maps). After that, both maps have been subtracted. The result is shown in Fig. 9, upper left, indicated as "Dataset 1 vs Dataset 2, 3 &4). In the rural case, directly with respect to each other. The results for the urban case, in absolute value, are shown in Fig. 9 for each dataset with respect to the rest and in Fig. 10 for the datasets grouped in pairs. The measurement points indicated on each map correspond to the first of the sets or groups of sets referred to in the legend.

In the urban area, the difference maps of a subset with respect to the rest, as shown in Fig. 9, confirm the differences around the BTS's, especially when the compared subset does not have LOS measurements

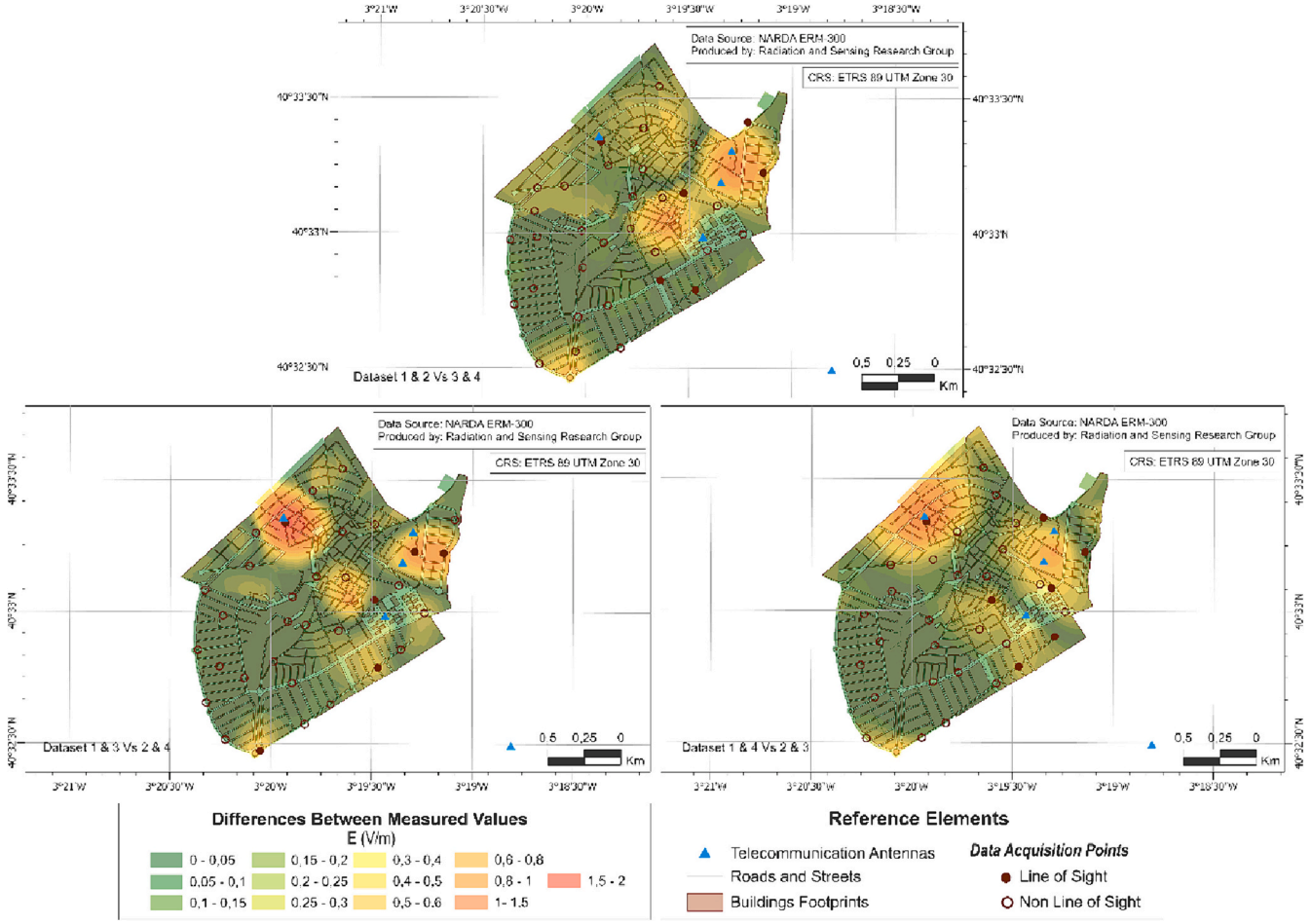

Fig. 10. Differences between pairs of datasets.

near them. In contrast, in the shaded coverage areas to the west, regardless of the chosen subset, the differences are very low. When considering a pair of the subsets against each other (Fig. 10), the differences between interpolated areas and fixed points measured values are maximised.

In the rural case, the first difference observed when analysing Fig. 11 is that both maps are much more like each other than in the case of urban datasets since the observed differences are smaller. This is also corroborated by the statistical values shown in Table 2 and Fig. 4. The difference between values of the two interpolations is smaller when the covered area lacks LOS areas, while the differences are larger, as in the urban case, when no sampling takes place in the vicinity of the BTS's or there are unsampled LOS areas.

As can be seen in Table 1, the subsets chosen in the urban area have an average distance between points (300–350 m) slightly lower than the ITU recommendation (500 m). The results shown up to now suggest that it should probably be even smaller, but in any case, to discard this original value of 500 m (4 points/m^2); an additional measurement campaign has been carried out with these characteristics.

An additional dataset of measurements consisting of eleven urban points (approximately 4 points/km^2) independent of the previous ones has been carried out. The range of measured values is between 0.08 and 2.39 v/m. The mean value is 0.407 and the standard deviation 0.671 fitted to a lognormal distribution. As in the previous case, the maximum value is found in the vicinity of the northernmost base station located in the area. As can be seen from the map in Fig. 12, the low sampling defects lead to an IDW-like representation that does not correspond to the variability of the data seen in any of the original subsets. Therefore, it becomes clear that the generic conditions of 500-m square grids are insufficient to assess adequately an urban area.

4. Discussion

As previously indicated, the measurement methodology follows the six-minute averaging procedure currently in force, although modified by the latest ICNIRP recommendations. These changes are mainly motivated by the deployment of 5G technology and the consequent change in the time variation of the radiated signals. In the case of the population analysed, the deployment of this technology has not yet taken place, so the measurement procedure can be considered adequate. The incorporation of the new network may imply modifications in the way in which the exposure value is obtained in the chosen point, but in the same way there will be a measured value to interpolate in the area under study. In the choice of locations and measurement points, the LOS criterion is independent of the type of technology to be considered. From a radio wave propagation point of view, the frequencies used (not the temporal shape of the signals) for the new 5G network are not significantly different from those of the current ones, so the basic propagation mechanisms (LOS or multipath) will be similar. Although this will require further analysis, the criteria chosen for the definition of the points should be comparable. Another possible factor to consider in subsequent analyses is the typology of buildings (in the case under study they are mainly residential areas). In the comparison with other previous works, it should be noted that most of the analysed works use personal exposure meters to obtain the exposure values. This may lead to differences in the reported values since, as noted, exposure meters tend to underestimate the actual exposure value (Martin-Castillo et al., 2021).

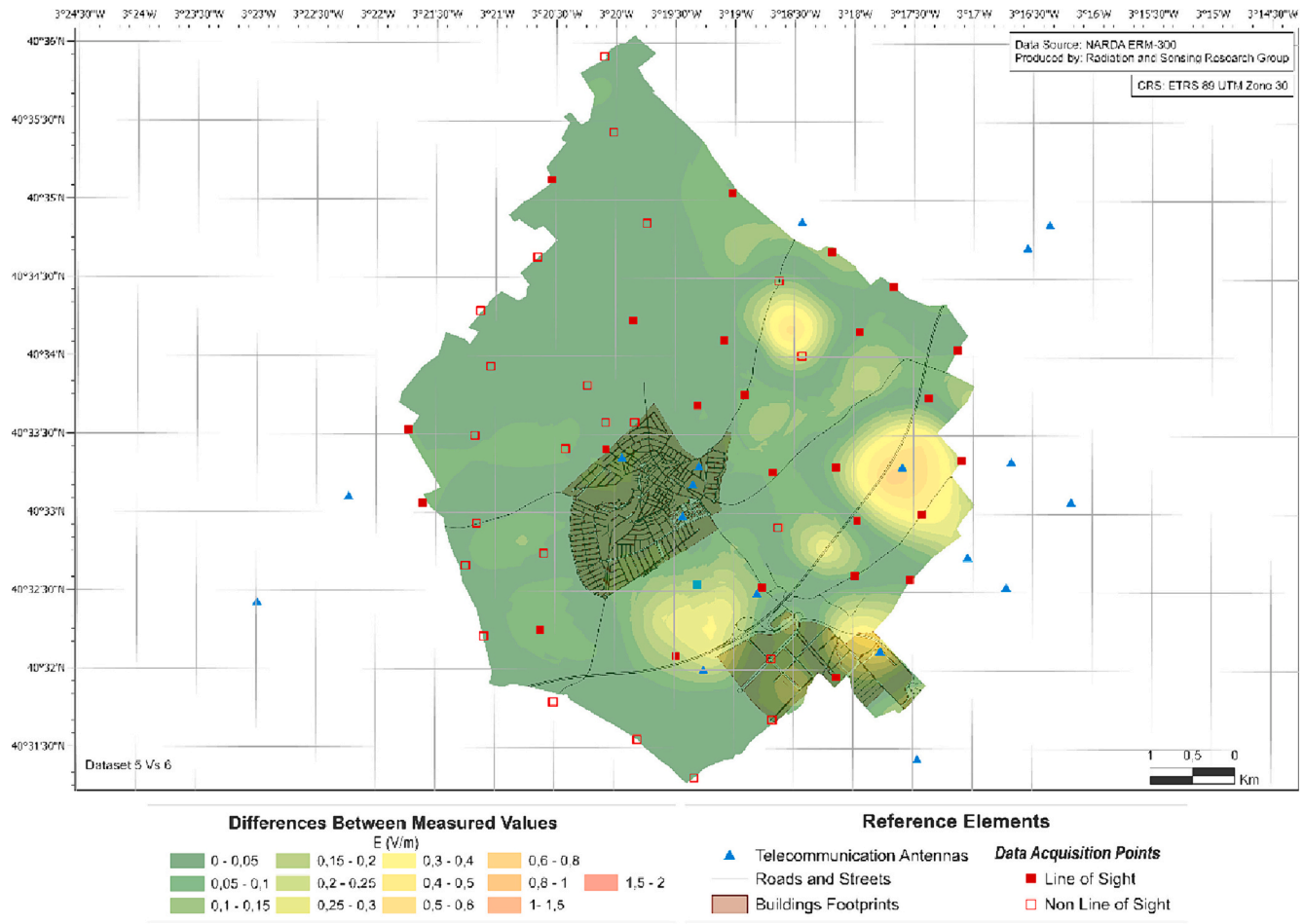

Fig. 11. Differences between rural datasets.

Considering the previous possible limitations, as can be seen in Fig. 5, in general, when the measurements are carried out under LOS conditions and near the emitting source, as expected, the highest values are obtained. The existence of LOS to the BTS's of the municipality is what fundamentally determines the levels of exposure. Fig. 7, in the map corresponding to dataset 1, shows an area with a higher level to the north, which is not visible in the rest of the maps due to the lack of sampling in LOS conditions and proximity to the base station in those sets. On the contrary, in dataset 2 the measurement points defined as LOS are relatively far from the emitting sources, which results in an underestimation of a large part of the surface and a more homogeneous level map, which does not detect the areas with higher levels. This highlights the importance of collecting points on the surface under study near the emitters and under LOS conditions. In contrast, in shaded areas, the position of the measurement point has less influence on obtaining a similar representation of the interpolated levels. In the four cases shown in Fig. 7, similar levels can be seen in the western area. An additional issue is the placement of measurement points on the perimeter of the area to be determined. When the area to be measured has points on the perimeter (datasets 2 and 3 in the western area), its surroundings show less variability. This should be an additional criterion for maintaining the accuracy at the limits of the area to be characterised.

Considering the difference maps in Fig. 9, the one with the smallest differences in the kriging interpolation with respect to the rest is the one corresponding to dataset 3. In other words, this subset has both statistical and geographical characteristics equivalent to the other three. Therefore, a quasi-optimal grid seems to exist for urban environments in terms of measurement campaign effort with a density of about 6 points/km^2 and an average distance between them of 350 m. This distance between points is significantly smaller than that expressed in the ITU K-113 recommendation (500 m and 4 points/km^2). This subset does not contain the maximum measured value, as it does not sample near the northernmost base station, suggesting that some additional points should be incorporated to increase its point density.

When increasing the point density by grouping the subsets in pairs (Fig. 10) the best results are achieved when combining heterogeneous sets (dataset 1 and 2), especially around base stations. That is, reiterating measurements in direct viewing areas around an emitting source does not increase the statistical significance of the set. On the contrary, combining measurements in N-LOS and LOS condition does improve the representativeness of the dataset. Therefore, the point density for an optimal grid must be established taking into account whether the surface to be assessed has predominantly LOS or N-LOS characteristics or whether, on the contrary, both conditions are balanced. This shows that the criterion of increasing the number of measurements in areas where both conditions coexist should be considered.

Therefore, if we consider the grids shown in Fig. 6 (250 m and 16 points/km^2), it could be established that, in those grids where there is an emitting source, a measurement point must be located under direct vision conditions. On the other hand, in those where there is no emitting source, considering the homogeneity of the surface with respect to the conditions of LOS and N-LOS, could be grouped with the adjacent ones to reduce the number of measurements necessary, without a priori implying a loss of statistical significance. Considering the initial distances (250 m) and the distance detected in dataset 3 (350 m), the level of grid grouping should be set at a value of two, and in any case, less than three. Having made this argument, it would remain, as future work, to evaluate the grouping techniques that allow this process to be

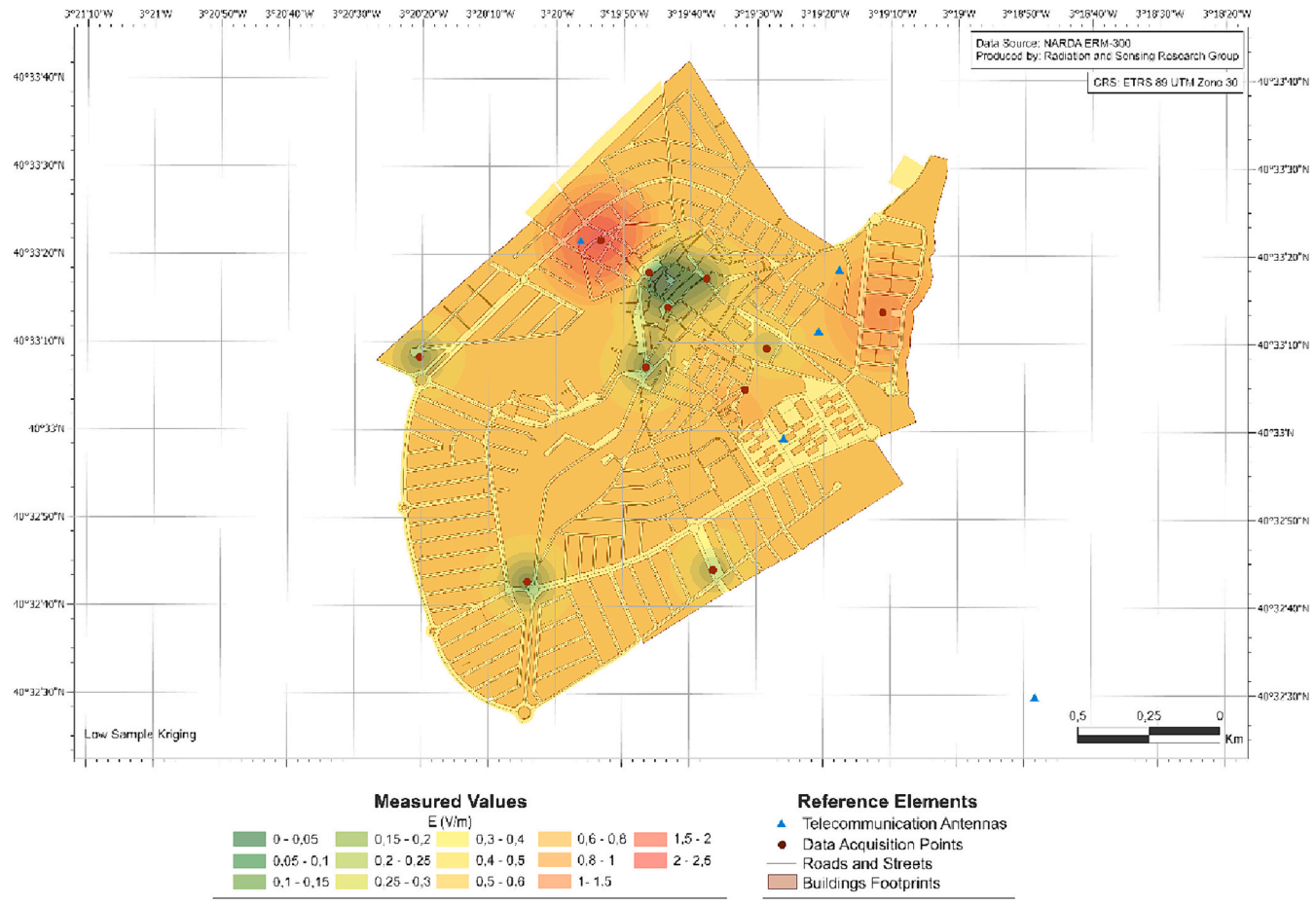

Fig. 12. Data representation with a reduced set of points.

automated. According to the results shown and taking into account what has been said for the particular analysis of the sources, the average density of points can be increased with respect to the case of dataset 3, so that the average values would be around 300 m and 8 points/km^2.

In the rural area, the topography of the terrain mainly determines the areas of LOS and N-LOS. The north-western part of the municipality is mainly in shadow, and the south-eastern part is in direct vision. Because of this, there is a correlation between the viewshed analysis of the emitting sources (Fig. 6), the topography of the terrain (Fig. 1) and the representation of measured values (Fig. 5). The major differences between the two maps in Fig. 11 correspond to the existence of measurements in the vicinity of the emission sources (to the east) or associated with the under- or oversampling of different areas (to the south). An effect is seen in the case of set 6 (higher point density) leading to the appearance of island zones similar to the representation of an inverse distance-style interpolation in Fig. 12. Therefore, over the reference distance of 500 m between points, an increase of at least 50% (750 m) could be considered without any significant statistical loss of the set, except for respecting the sampling in the LOS areas. The grouping of grids into homogeneous zones would also be possible, as in the urban case. Here, also starting from base grids of 250 m on each side, it would be foreseeable to reach a level of grouping of up to 4–8 grids of homogeneous characteristics to be assessed with a single measurement.

Finally, to check the validity of the proposal, a third set of urban measurements in 2023, independent of the previous ones, was carried out in the area under analysis. Based on the criterion of eight points/km^2, measurements were taken at the sites indicated at the top of Fig. 13. The campaign consists of 27 points, of which 14 were measured under LOS conditions and 13 under N-LOS conditions. The range of measured values was between 0.05 and 1.65. The average distance between points is 272 m. The set has a mean value of 0.418 and a standard deviation of 0.570. Comparing these values with those of the original set, they are slightly higher (Table 2 and Fig. 14), because of a higher ratio of points measured in LOS conditions. The lognormal distribution fit of both data sets is shown in Fig. 15. The *p*-value of the mean indicates that there is no significant statistical difference between the two sets, but the p-value of the variance does. In other words, both sets are able to statistically represent the mean value of the municipality, although obviously, a larger number of samples reflects differently the variability of these measures.

If we now compare the differences between the two sets of measurements (Fig. 13 bottom right) we can see a predominance of green tones that represent the lowest absolute error values between the kriging interpolations of both sets. Comparing this result with those in Fig. 9 and Fig. 10, where the original subsets were subtracted, a larger green area is visible. Therefore, the reduction from 65 to 27 values (23.21 points/km^2 to 9.64 points/km^2) has resulted in an equivalent mean representation and a surface distribution with small errors. This value of point density is slightly higher than the initially proposed value of 8 points/km^2 and 300 m distance between points and it is due to the irregularity of the measured surface and the necessity to sample on the perimeter of the surface to reduce the variability in the limits. Regarding the LOS conditions established in the visual watershed analysis, of the Fifty-seven urban grids of 250 × 250 m^2, twenty-seven have been sampled, which is equivalent to 47% of the total (overall reduction of 2:1). Nineteen of the measurements were made in one of the twenty-four grids marked above 50% in the visual viewshed analysis in Fig. 6 (5:4 clustering). In contrast, only eight measurements were made in any of the thirty-tree grid squares below 50% (4:1 clustering).

These results can also be related to the grid size in an equivalent way.

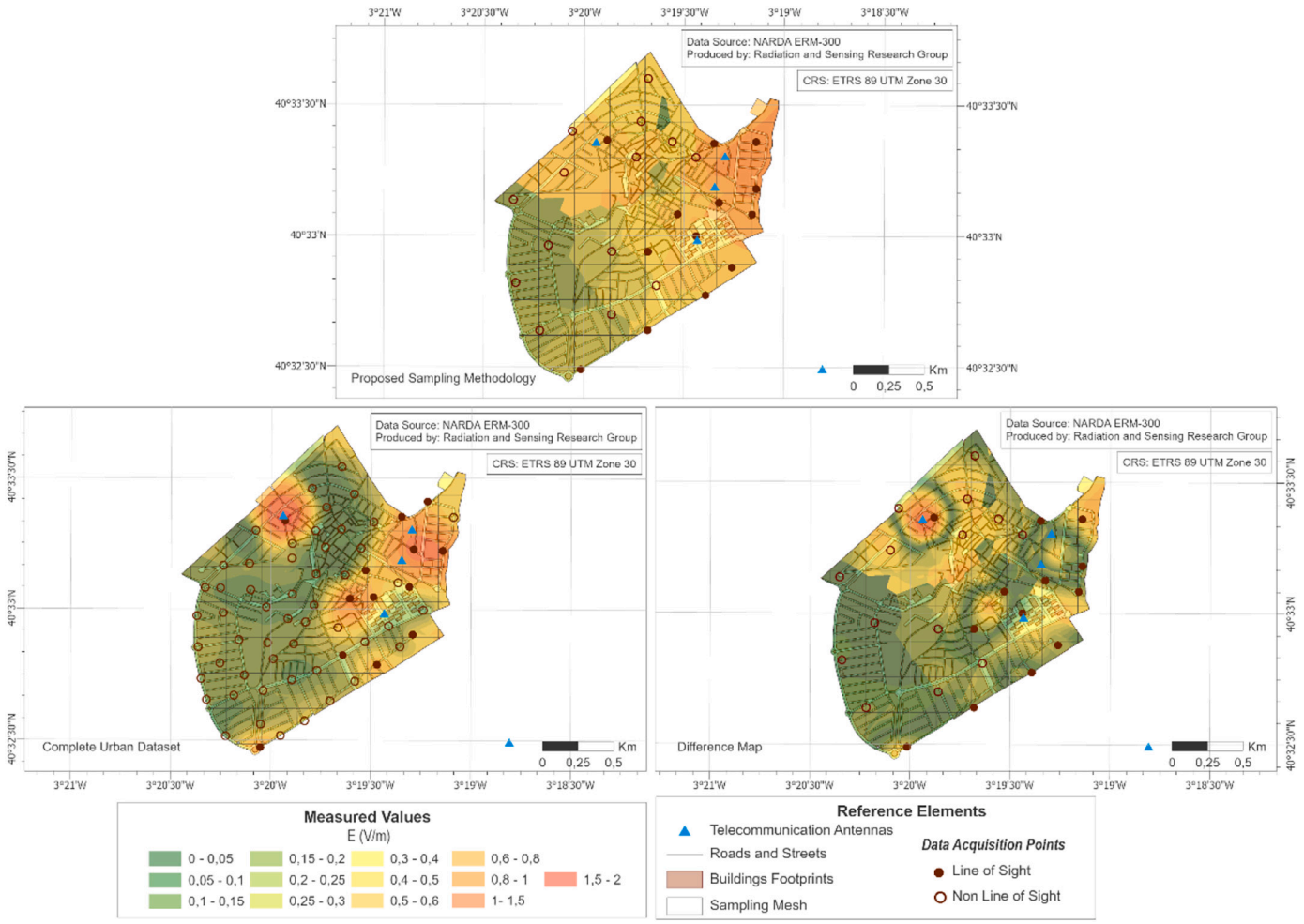

Fig. 13. Representation of the new dataset of points (top), original urban dataset (bottom left) and the difference between them (bottom right).

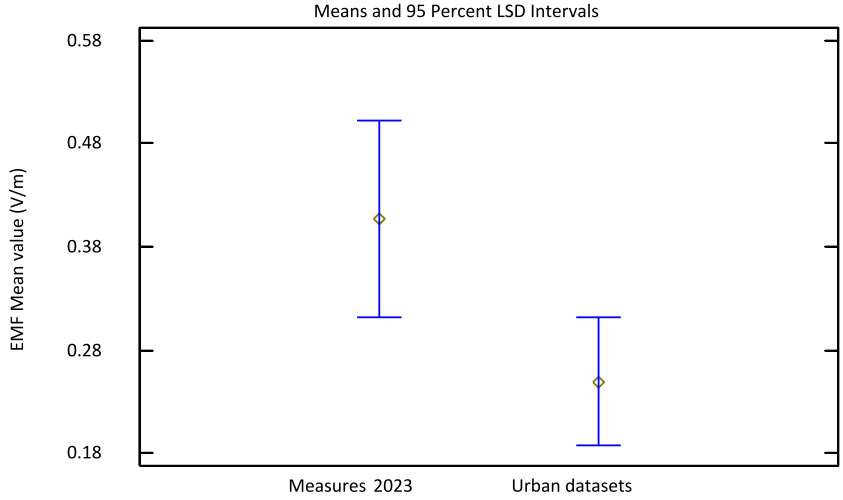

Fig. 14. EMF Mean values of the new dataset (Measures 2023) of points and of the original urban dataset.

Under LOS conditions, the recommended grid size for an urban area should not exceed 250 m on a side to assess the sampling area. On the other hand, when the area to be assessed does not have LOS points, the grid size can be up to 500 × 500 m^2. Each grid of 500 × 500 m^2 contains 4 grids of 250 × 250 m^2, which is equivalent to a grouping of 4:1. In addition to this, in the rural area, where multipath propagation does not exist, these distances can be increased to values of 700 m between points as previously deduced, which would lead to a clustering of approximately 2:1 of the 500 × 500 m^2 grids (6–8 in 250 × 250 m^2 grids).

The original and 2023 datasets of measurements also show a slight average difference between them as can be seen in Figs. 14 and 15. The latter measurements have an average value of approximately 0.42 V/m

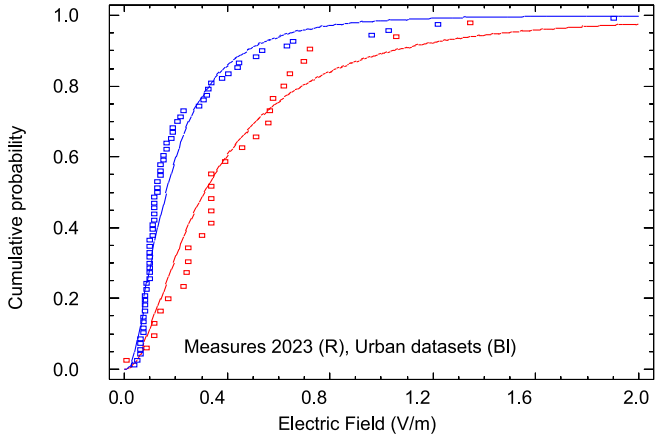

Fig. 15. Adjustment of the distributions of the 2023 set of points (red) and the original urban set (blue). (For interpretation of the references to colour in this figure legend, the reader is referred to the web version of this article.)

and the former of 0.25 V/m. This difference may have been influenced by two main causes. The first is obviously a higher level of EMF and the second, a higher proportion of measurements in LOS conditions (14/27 in the latter and 13/65 in the former) and therefore of higher value. This result reaffirms that, if LOS measurements are not properly incorporated, the mean value obtained is underestimated in the area under study.

5. Conclusions

In this proposal, the methodology for EMF exposure mapping in large areas has been analysed. To optimize the measurement effort over a large area, a division into 250 × 250 m^2 urban grids should be considered, in which the possible sources of radiation should be known. A measurement under LOS conditions must be performed in each of the grids in which any of the emitters is present. The absence of measurements under LOS conditions implies an underestimation of the mean values. To select the rest of the grids to be measured, the viewshed analysis allows to simplify the number of measurements by grouping those grids determined as N-LOS. To achieve optimal interpolation results over the entire surface, sufficient measurements must also be available on its perimeter. Interpolation by ordinary stable kriging obtains adequate results under LOS and N-LOS conditions. The generated maps contribute to a better perception of risk as they provide an objective and simple tool to show the level of EMF. They do not require complex propagation models but are based on interpolations made within a GIS. They can also be combined, using these techniques, for risk assessment and even, if epidemiological data are available, for possible correlations studies.

The proposal considers the differences between urban areas, with the possibility of multipath, and rural (non-urban) areas. For the analysis of urban areas, a grid of 250 × 250 m^2 has been proposed as a guideline for the spatial organisation of the territory in urban areas and 500 × 500 m^2 in rural areas.

Depending on the extent and regularity of the surface, the density of measurement points has been estimated to be between 8 and 10 points per square kilometre in the urban area. Lower point densities result in IDW representations and higher densities increase the measurement effort excessively. In the case under study, for the urban area, a density of 9.64 points/km^2 has been reached.

The study has been performed following the six-minute averaging criterion and in a bandwidth from 100 kHz to 3 GHz. The latest ICNIRP recommendations modify these values to take into account, among others, the new 5G signals, not yet present in the area. The urban study was carried out in a mainly residential area, where there are no concentrations of the general public, which could lead to areas of greater exposure due to greater use of the network. For future studies, therefore, the measurement and comparison according to the latest ICNIRP recommendations is still pending in areas where the new 5G networks have been incorporated and in urban micro-environments where there is a higher population density or uses significantly different from residential. Another point of continuation of this research is the correlation of the measured values with tumor statistics and other diseases. The opportunity provided by exposure maps created for entire urban environments may allow, where appropriate, to find possible relationships.

Funding

This work was supported by the University of Alcala and Comunidad de Madrid [grant numbers CM/JIN/2021-032, UAH INFR. B 2021-012 and CM/JIN/2019-036].

These research projects are founded by the University of Alcalá and Comunidad de Madrid (Government of Madrid Region) in a competitive concurrence and external evaluation basis. The projects have been developed from 2017 to 2023.

Declaration of competing interest

The authors declare that they have no known competing financial interests or personal relationships that could have appeared to influence the work reported in this paper.

Data availability

Data will be made available on request.

References

Aerts, S., Deschrijver, D., Verloock, L., Dhaene, T., Martens, L., Joseph, W., 2013 Oct. Assessment of outdoor radiofrequency electromagnetic field exposure through hotspot localization using kriging-based sequential sampling. Environ. Res. 126, 184–191.

Beekhuizen, J., Vermeulen, R., Kromhout, H., Bürgi, A., Huss, A., 2013. Geospatial modelling of electromagnetic fields from mobile phone base stations. Sci. Total Environ. 445, 202–209.

Beekhuizen, J., Vermeulen, R., van Eijsden, M., van Strien, R., Bürgi, A., Loomans, E., et al., 2014 Jun. Modelling indoor electromagnetic fields (EMF) from mobile phone base stations for epidemiological studies. Environ. Int. 67, 22–26.

Biasotto, L.D., Kindel, A., 2018. Power lines and impacts on biodiversity: A systematic review. In: Environmental Impact Assessment Review, vol. 71. Elsevier Inc, pp. 110–119.

BOE, 2001. Real Decreto 1066/2001. por el que se aprueba el Reglamento que establece las condiciones de protección del dominio público, restricciones a las emisiones radioeléctricas y medidas de protección sanitaria frente a emisiones radioeléctricas. s.l. [Internet]. BOE Num.234, pp. 36217–36227. Available from: https://www.boe.es/boe/dias/2001/09/29/pdfs/A36217-36227.pdf.

BOE, 2002. Orden CTE/23/2002. por la que se establecen condiciones para la presentación de determinados estudios y certificaciones por operadores de servicios de radiocomunicaciones. s.l. [Internet]. BOE Num.11, pp. 1528–1536. Available from: https://www.boe.es/boe/dias/2002/01/12/pdfs/A01528-01536.pdf.

Bojdova, V., Skurcak, L., Bojda, P., Rybanský, L., 2019. Broadband Monitoring Measurements Analysis to Find the Main Sources Determining the Temporal Trend of Population Exposure in Slovakia.

Bolte, J.F.B., 2016. Lessons learnt on biases and uncertainties in personal exposure measurement surveys of radiofrequency electromagnetic fields with exposimeters. In: Environment International, vol. 94. Elsevier Ltd, pp. 724–735.

Cansiz, M., Abbasov, T., Kurt, M., Celik, A., 2016 Mar. Mapping of radio frequency electromagnetic field exposure levels in outdoor environment and comparing with reference levels for general public health. J. Expo. Sci. Environ. Epidemiol. 28.

Čučković, Z., 2021. QGIS Visibility Analysis [Internet] [cited 2024 Mar 27]. Available from: https://github.com/zoran-cuckovic/LandscapeArchaeology.org.

ESRI, 2016. ArcGIS PRO [Internet] [cited 2024 Mar 27]. Available from: https://www.esri.com/en-us/arcgis/products/arcgis-pro/overview.

European Union, 1999. Council Recommendation of 12 July 1999 on the limitation of exposure of the general public to electromagnetic fields (0 Hz to 300 GHz). 1999/519/EC Official Journal, pp. 59–70.

Frei, P., Mohler, E., Bürgi, A., Fröhlich, J., Neubauer, G., Braun-Fahrländer, C., et al., 2009. A prediction model for personal radio frequency electromagnetic field exposure. Sci. Total Environ. [Internet] 408 (1), 102–108. Available from: https://www.sciencedirect.com/science/article/pii/S0048969709008675.

Gajšek, P., Ravazzani, P., Wiart, J., Grellier, J., Samaras, T., Thuroczy, G., 2013 Mar. Electromagnetic field exposure assessment in Europe radiofrequency fields (10 MHz-6 GHz). J. Expo. Sci. Environ. Epidemiol. 1–8.

Giliberti, C., Boella, F., Bedini, A., Palomba, R., Giuliani, L., 2009. Electromagnetic mapping of urban areas: the example of Monselice (Italy). PIERS Online 5 (1), 56–60.

Gonzalez-Rubio, J., Najera, A., Arribas, E., 2016 Aug 1. Comprehensive personal RF-EMF exposure map and its potential use in epidemiological studies. Environ. Res. 149, 105–112.

Gonzalez-Rubio, J., Arribas, E., Ramirez-Vazquez, R., Najera, A., 2017 Dec 1. Radiofrequency electromagnetic fields and some cancers of unknown etiology: an ecological study. Sci. Total Environ. 599–600, 834–843.

International Commission on Non-Ionizing Radiation Protection (ICNIRP), 1998. Guidelines for limiting exposure to time-varying electric, magnetic, and electromagnetic fields (up to 300 GHz). Health Phys. 74 (4), 494–522.

International Commission on Non-Ionizing Radiation Protection (ICNIRP), 2020. Guidelines for limiting exposure to electromagnetic fields (100 kHz to 300 GHz). Health Phys. [Internet] 118 (5). Available from: https://journals.lww.com/health-physics/fulltext/2020/05000/guidelines_for_limiting_exposure_to.2.aspx.

International Electrotechnical Commission, 2019. IEC TR 62669:2019. Case studies supporting IEC 62232 - Determination of RF field strength, power density and SAR in the vicinity of radiocommunication base stations for the purpose of evaluating human exposure [Internet] [cited 2024 Mar 27]. Available from: https://webstore.iec.ch/publication/62014.

International Telecommunication Union, 2018. Recommendation ITU-T K.61: Guidance to measurement and numerical prediction of electromagnetic fields for compliance with human exposure limits for telecommunication installations [Internet] [cited 2024 Mar 27]. Available from: https://www.itu.int/rec/T-REC-K.61/en.

International Telecommunication Union, 2024. Recommendation ITU-T K.83 : Monitoring of electromagnetic field levels [Internet] [cited 2024 Mar 27]. Available from: https://www.itu.int/rec/T-REC-K.83-202401-P/en.

International Telecommunication Union. Recommendation ITU-T K.100, 2021. Measurement of radio frequency electromagnetic fields to determine compliance with human exposure limits when a base station is put into service [Internet] [cited 2024 Mar 27]. Available from: https://www.itu.int/rec/T-REC-K.100-202106-I/en.

International Telecommunication Union. Recommendation ITU-T K.113, 2015. Generation of radiofrequency electromagnetic field level maps [Internet] [cited 2024 Mar 27]. Available from: https://www.itu.int/rec/T-REC-K.113-201511-I/en.

Iyare, R., Volskiy, V., Vandenbosch, G., 2018 Mar. Study of the correlation between outdoor and indoor electromagnetic exposure near cellular base stations in leuven, Belgium. Environ. Res. 168.

Jawad, O., Lautru, D., Benlarbi-Delai, A., Dricot, J.M., Doncker, P., 2014 Mar. Study of human exposure using kriging method. Progr. Electromagnet. Res. B 61, 241–252.

Koppel, T., Ahonen, M., Carlberg, M., Hardell, L., 2022. Very high radiofrequency radiation at Skeppsbron in Stockholm, Sweden from mobile phone base station antennas positioned close to pedestrians' heads. Environ. Res. [Internet] 208, 112627. Available from: https://www.sciencedirect.com/science/article/pii/S0013935121019289.

Kross, A., Kaur, G., Jaeger, J.A.G., 2022 Nov 1. A geospatial framework for the assessment and monitoring of environmental impacts of agriculture. Environ. Impact Assess. Rev. 97.

Liu, J., Shi, S., Li, H., Wei, M., Mei, N., Wang, X., et al., 2019. Research on the distribution of the regional electromagnetic radiation based on the interpolation methods. In: 2019 International conference on microwave and millimeter wave technology (ICMMT), pp. 1–3.

Martens, A., Slottje, P., Meima, M., Beekhuizen, J., Timmermans, D., Kromhout, H., et al., 2016 Mar. Residential exposure to RF-EMF from mobile phone base stations: model predictions versus personal and home measurements. Sci. Total Environ. 550, 987–993.

Martin-Castillo, S., Gonzalez-Rubio, J., Najera, A., Lopez-Espi, P.L., 2021. Personal exposure to RF-EMF prior to the deployment of the 5th generation of mobile telephony: Map of a whole city. In: The Joint Annual Meeting of the Bioelectromagnetics Society and the European BioElectromagnetics Association BIOEM21. Ghent.

Najera, A., Alpuente-Hermosilla, J., González-Rubio, J., Sánchez-Montero, R., López-Espí, P.L., 2018. Exposure to radiofrequency electromagnetic fields (RF-EMF) assessment: Comparison between spot and personal exposimeter measurements in Tarancón (Spain). In: The Joint Annual Meeting of the Bioelectromagnetics Society and the European BioElectromagnetics Association, BIOEM18. Slovenia.

Neubauer, G., Feychting, M., Hamnerius, Y., Kheifets, L., Kuster, N., Ruiz, I., et al., 2007. Feasibility of future epidemiological studies on possible health effects of mobile phone base stations. Bioelectromagnetics [Internet] 28 (3), 224–230. Available from: https://onlinelibrary.wiley.com/doi/abs/10.1002/bem.20298.

Pachón-García, F.T., Jiménez-Barco, A., Paniagua-Sánchez, J.M., Rufo-Pérez, M., 2014. New approach based on ANN and RBF for analyzing the spatial distribution of electromagnetic field from an exposure standpoint. Neural Comput. Appl. [Internet] 25, 1479–1494. Available from: https://api.semanticscholar.org/CorpusID:254029455.

Ramirez-Vazquez, R., Gonzalez-Rubio, J., Arribas, E., Najera, A., 2019. Personal RF-EMF exposure from mobile phone base stations during temporary events. Environ. Res. 175, 266–273. Aug 1.

Reis, A.L., Rego, C.G., Lopez, D.C.T., Nunes, M.L., 2018. A comparative study for radioelectric coverage models applied to mobile communicaton systems performance analysis. In: 2018 IEEE-APS Topical Conference on Antennas and Propagation in Wireless Communications (APWC), pp. 746–749.

Röösli, M., Hertach, P., Mohler, E., Hug, K., 2010 Mar. Systematic review on the health effects of exposure to radiofrequency electromagnetic fields from mobile phone base stations. Bull. World Health Organ. 88, 887–896F.

Sagar, S., Dongus, S., Schoeni, A., Roser, K., Eeftens, M., Struchen, B., et al., 2018. Radiofrequency electromagnetic field exposure in everyday microenvironments in Europe: a systematic literature review. J. Expo Sci. Environ. Epidemiol. [Internet] 28 (2), 147–160. Available from: https://doi.org/10.1038/jes.2017.13.

Sánchez-Montero, R., Alén-Cordero, C., López-Espí, P.L., Rigelsford, J.M., Aguilera-Benavente, F., Alpuente-Hermosilla, J., 2017. Long term variations measurement of electromagnetic field exposures in Alcalá de Henares (Spain). Sci. Total Environ. 598.

Statgraphics Technologies Inc, 2009. Statgraphics® Centurion XVI User Manual. Statgraphics. Available from: http://www.statgraphics.com/resources-downloads.

Thuróczy, G., Molnár, F., Jánossy, G., Nagy, N., Kubinyi, G., Bakos, J., et al., 2008 Feb. Personal RF exposimetry in urban area. Ann. Telecommun. 63 (1–2), 87–96.

Urbinello, D., Huss, A., Beekhuizen, J., Vermeulen, R., Röösli, M., 2014 Jan. Use of portable exposure meters for comparing mobile phone base station radiation in different types of areas in the cities of Basel and Amsterdam. Sci. Total Environ. 468–469, 1028–1033.

Urbinello, D., Joseph, W., Huss, A., Verloock, L., Beekhuizen, J., Vermeulen, R., et al., 2014b. Radio-frequency electromagnetic field (RF-EMF) exposure levels in different European outdoor urban environments in comparison with regulatory limits. Environ. Int. 68, 49–54.

Vermeeren, G., Markakis, I., Goeminne, F., Samaras, T., Martens, L., Joseph, W., 2013. Spatial and temporal RF electromagnetic field exposure of children and adults in indoor micro environments in Belgium and Greece. Prog. Biophys. Mol. Biol. [Internet] 113 (2), 254–263. Available from: https://www.sciencedirect.com/science/article/pii/S0079610713000576.

Viel, J.F., Tiv, M., Moissonnier, M., Cardis, E., Hours, M., 2011. Variability of radiofrequency exposure across days of the week: a population-based study. Environ. Res. 111 (4), 510–513.

Wang, Y., Shen, C., Bartsch, K., Zuo, J., 2021 Mar 1. Exploring the trade-off between benefit and risk perception of NIMBY facility: a social cognitive theory model. Environ. Impact Assess. Rev. 87.